

Blending the Evaporation Precipitation Ratio with the Complementary Principle Function for the Prediction of Evaporation

Zhang Lu¹ and Wilfried Brutsaert²

¹CSIRO Land and Water

²Cornell University

November 23, 2022

Abstract

One class of descriptions of landscape evaporation is based on the principle that actual evaporation E and atmospheric evaporative demand exhibit complementary behavior. A feature of some recent implementations of this approach is the need for the estimation of a free parameter, usually by calibration. In a different class of representations of landscape evaporation, several functional forms have been proposed in the past for the dependency of the annual evaporation precipitation ratio (E/P) on the annual aridity index - the Schreiber-Oldekop hypothesis, also known as the Budyko framework. While there is no general agreement in the literature on the optimal formulation of the “maximum possible evaporation”, the functional forms appear to be quite insensitive to its exact nature. This observation allows to be equated with the evaporative demand, and this immediately leads to a blending of the annual evaporation precipitation ratio (E/P) with the complementary evaporation principle, and the prediction of its unknown free parameter. As this free parameter is found to be relatively insensitive to time scale, the complementary functions become not only calibration-free at the annual time scale, but also applicable even at daily time scales. The results are shown to be applicable worldwide with experimental data from 516 catchment water balance set-ups and 152 high quality eddy covariance flux stations. The present approach offers a practical tool for the prediction of daily evaporation using only routine meteorological data such as air temperature, humidity, wind speed, net radiation, and long-term average precipitation.

1 **Blending the Evaporation Precipitation Ratio with the Complementary Principle**
2 **Function for the Prediction of Evaporation**

3
4 Lu Zhang

5 CSIRO Land and Water, Canberra, Australian Capital Territory, Australia

6
7 Wilfried Brutsaert

8 School of Civil and Environmental Engineering, Cornell University, Ithaca, New York, USA

9 (1/02/2021)

10
11 **Abstract**

12 One class of descriptions of landscape evaporation is based on the principle that actual
13 evaporation E and atmospheric evaporative demand E_{pa} exhibit complementary behavior. A
14 feature of some recent implementations of this approach is the need for the estimation of a
15 free parameter, usually by calibration. In a different class of representations of landscape
16 evaporation, several functional forms have been proposed in the past for the dependency of
17 the annual evaporation precipitation ratio (E/P) on the annual aridity index (E_{\max} / P) - the
18 Schreiber-Oldekop hypothesis, also known as the Budyko framework. While there is no
19 general agreement in the literature on the optimal formulation of the “maximum possible
20 evaporation” E_{\max} , the functional forms of $(E/P) = f(E_{\max} / P)$ appear to be quite
21 insensitive to its exact nature. This observation allows E_{\max} to be equated with the
22 atmospheric evaporative demand E_{pa} , and this immediately leads to a blending of the annual
23 evaporation precipitation ratio (E/P) with the complementary evaporation principle, and the
24 prediction of its unknown free parameter. As this free parameter is found to be relatively
25 insensitive to time scale, the complementary functions become not only calibration-free at the
26 annual time scale, but also applicable even at daily time scales. The results are shown to be
27 applicable worldwide with experimental data from 524 catchment water balance set-ups and
28 156 high quality eddy covariance flux stations. The present approach offers a practical tool
29 for the prediction of daily evaporation using only routine meteorological inputs including air
30 temperature, specific humidity, wind speed, net radiation, and long-term average precipitation.

31 **1. Introduction**

32 As an important natural process, evaporation from the land surface has been studied
33 extensively and various methods have been developed (Brutsaert, 1982, 2005; Wang and
34 Dickinson, 2012; McMahon et al., 2013). One class of more practical methodologies for
35 estimating evaporation is based on the well-known complementarity between actual
36 evaporation E and atmospheric evaporative demand, also known as apparent potential
37 evaporation E_{pa} . This complementary principle has been used in various ways to estimate
38 evaporation at temporal scales ranging from hourly, to mean annual (Brutsaert and Stricker,
39 1979; Morton, 1983, Lemeur and Zhang, 1990; Parlange and Katul, 1992; Hobbins et al.,
40 2001). Over the years the basic complementarity idea has been further generalized (e.g.
41 Brutsaert and Parlange, 1998; Brutsaert, 2015) and this has enhanced an understanding of the
42 underlying assumptions and has provided it a stronger base. The input data required by these
43 more recent implementations of the complementary principle can be readily obtained from
44 meteorological stations. However, their application still requires the estimation of at least one
45 model parameter. Different ad-hoc methods have been used to deal with this issue, either by
46 introducing additional rescaling assumptions with contrived variables (e.g. Crago et al., 2016;
47 Crago and Qualls, 2018) or by calibrating the model parameters using measured evaporation
48 data (e.g. Kahler and Brutsaert 2006; Liu et al. 2016, 2018; Brutsaert et al. 2017, Zhang et al.
49 2017; Brutsaert et al. 2020).

50 Another widely used methodology for estimating mean evaporation E , but only at the mean
51 annual scale, is based on the Schreiber-Oldekop hypothesis, which makes use of maximum
52 possible evaporation E_{\max} and mean annual precipitation P . This hypothesis, which is also
53 commonly known as Budyko's framework, states that the evaporation precipitation ratio
54 (E / P) is a function of the aridity index (E_{\max} / P) (e.g. Budyko 1974; Zhang et al., 2001,
55 2004; Andréassian et al., 2016; Wang et al., 2016; Sposito, 2017). Some comparable features

56 of the Schreiber-Oldekop hypothesis and the complementary principle have been brought up
57 and examined before (e.g. Zhang et al. 2004; Yang et al., 2006; Zhou et al., 2015; Lhomme
58 and Moussa, 2016); but while these studies have greatly stimulated current understanding, so
59 far this has not led to tangibly practical procedures.

60 In brief, the present study was motivated by the idea that the complementary principle and the
61 evaporation precipitation ratio can be made to share a common variable, namely by equating
62 the atmospheric demand of the former with the maximum possible evaporation of the latter.
63 This way, the two methodologies become blended, and using their remaining input variables,
64 namely the equilibrium evaporation and the precipitation, respectively, the unknown
65 parameter can be estimated. Specifically, this study aims briefly to re-examine the
66 assumptions under these two approaches and to develop a method for estimating the annual
67 scale model parameter in the complementary principle. Because this parameter, coined β
68 herein, is relatively insensitive to time scale it can then be used to calculate evaporation from
69 routine meteorological data at any shorter time scale.

70

71 **2. Theoretical Framework**

72 2.1 The Evaporation Precipitation Ratio as a Function of Aridity Index

73 2.1.1 Background.

74 The search for general relationships among the main components of the annual water budget
75 of river basins has a long history. Among the earliest attempts to relate mean annual runoff R
76 with mean annual precipitation P in central Europe, Penck (1896) used a linear function,
77 whereas Ule (1903) adopted a cubic polynomial. Further inspection of Ule's data and
78 methodology by Schreiber (1904) "made him suppose" that an exponential function would be

79 feasible, as this form had been used in many other problems in physics and meteorology; thus
80 Schreiber proposed the following scaled relationship

$$81 \quad R / P = \exp(-k_s / P) \quad (1)$$

82 Here k_s in the exponent is a constant for a given river basin. By a series expansion of (1),
83 namely

$$84 \quad R = P - k_s + \frac{k_s}{2} \left(\frac{k_s}{P} \right) - \frac{k_s}{6} \left(\frac{k_s}{P} \right)^2 + \frac{k_s}{24} \left(\frac{k_s}{P} \right)^3 - \dots \quad (2)$$

85 Schreiber showed that k_s equals the value of the difference $(P - R)$ for very large P ; he
86 denoted this difference as the “remainder” or “leftover part”, which would start at zero for
87 $P = 0$, and asymptotically approach its maximal value k_s for large increasing P . He did not
88 further comment on the specific physical meaning of this remainder, nor on its maximal value.
89 Obviously, Schreiber’s remainder, which is the part of the mean annual precipitation that
90 does not run off, is in fact the mean annual evaporation from the basin. Schreiber was
91 undoubtedly aware of this, as he was familiar with Penck’s (1896) equation $(P - R) = E$,
92 whom he quotes in his paper. But it must not have occurred to him to call k_s the maximal
93 evaporation rate, because his study and also Ule’s were solely focused on runoff prediction
94 and not concerned with evaporation.

95 What was already implicit in Schreiber’s analysis, was made explicit a few years later by
96 Oldekop (1911) who formally identified $(P - R)$ as the mean annual evaporation E and, after
97 Schreiber’s series expansion, k_s as the “possible maximum evaporation”, say E_{\max} . Thus
98 with Oldekop’s stipulation, (1) would be reformulated for mean annual evaporation as:

$$99 \quad E / P = 1 - \exp(-E_{\max} / P) \quad (3)$$

100 To describe his evaporation data Oldekop did not adopt (3), but expressed (E / E_{\max}) as a
101 hyperbolic tangent function of (P / E_{\max}) instead. Subsequently Budyko (1958; 1974), using
102 the dimensionless variables of Schreiber and Oldekop, felt that the geometric mean of
103 Schreiber's exponential (3) and Oldekop's hyperbolic tangent would provide an even better
104 fit to the available data. But this was only the beginning of a proliferation of other functions
105 in terms of the same 3 variables, as intended improvements over the original functions of
106 Schreiber, Oldekop and Budyko; all of these functions were in the general form

$$107 \quad (E / P) = f(E_{\max} / P) \quad (4)$$

108 Note as an aside that the functional relationship (4) is often, as Oldekop did, also written in
109 an equivalent, and mutually convertible form with E_{\max} as repeating variable, instead of P ,
110 namely as

$$111 \quad (E / E_{\max}) = F(P / E_{\max}) \quad (5)$$

112 Because Schreiber and Oldekop are clearly at the origin of (4) and (5), it would stand to
113 reason that all these subsequent formulations would be referred to as resulting from the
114 Schreiber-Oldekop hypothesis or as part of the Schreiber-Oldekop framework. Yet invariably
115 these subsequent functions in the form of (4) or (5) are now referred to as belonging to the
116 "Budyko framework". One can only guess why this discrepancy arose, because Budyko
117 himself consistently gave credit to the two earlier authors; a major reason perhaps was that
118 only Budyko's work can be read in English translation and served as the only source of (4),
119 whereas the papers of Schreiber (1904) and Oldekop (1911) are only available in their
120 original version. In any event, the attribution of the framework based on (4) or (5) to Budyko
121 is another example of Stigler's (1980) law that "No scientific discovery is named after its
122 original discoverer." While it may be too late to stop or even slow the current nomenclature

123 advance of Budyko in the literature, it is never too late to try to correct mistaken practices of
 124 the past and give credit where credit is due. It is hoped that, if a name must be attached to it,
 125 henceforth (4) and (5) will also be acknowledged as the Schreiber-Oldekop hypothesis.

126

127 2.1.2 Present Implementation.

128 Reviews of the several implementations of (4) and (5), that have appeared in the literature
 129 after Budyko can be found in Andreassian et al. (2016), Andreassian and Sari (2019), Wang
 130 et al. (2016), and Sposito (2017), among others. Although these equations differ in their
 131 functional form, their numerical relationships are very similar. For the purpose of the present
 132 study it was decided to work with the function first derived by Tixeront (1964) and later by
 133 Fu (1981; Zhang et al., 2004) by a different analytical method; this function can be written in
 134 terms of the original variables of (4), as follows

$$135 \quad \frac{E}{P} = 1 + \frac{E_{\max}}{P} - \left[1 + \left(\frac{E_{\max}}{P} \right)^w \right]^{1/w} \quad (6)$$

136 or, alternatively, in its equivalent form (5), as

$$137 \quad \frac{E}{E_{\max}} = 1 + \frac{P}{E_{\max}} - \left[1 + \left(\frac{P}{E_{\max}} \right)^w \right]^{1/w} \quad (7)$$

138 Here w is a model parameter, which is introduced for added flexibility; its estimation will be
 139 dealt with below in Section 4.1.1.

140 So far, the exact nature of this “possible maximum evaporation”, E_{\max} , has not been
 141 specified. In the literature on the Schreiber-Oldekop hypothesis various definitions have been
 142 implemented and there is still no consensus on its precise meaning, nor on the optimal

143 method of its estimation. Budyko (1974) originally put it equal to the net radiation.
144 Subsequently, it has been considered as the potential evaporation in some studies and as the
145 atmospheric evaporative demand or the apparent potential evaporation in others. For example,
146 in a survey of some 50 studies dealing with various implementations of (4) and (5), we found
147 that E_{\max} was implemented by net radiation in 14%, by the Priestley-Taylor equation in 26%,
148 by the Penman and related equations in 41%, by pan evaporation (MOPEX) in 14%, and by
149 temperature-based expressions in 5% of this admittedly limited sample. Thus put differently,
150 E_{\max} was represented by approximations of the true potential evaporation E_{po} in about 40%,
151 and by estimates of the apparent potential evaporation, or the atmospheric evaporative
152 demand E_{pa} in about 60% of the studies in this sample. As shown in what follows, for the
153 present purpose it will be found suitable to assume that $E_{\max} = E_{pa}$ in (6) and (7).

154 2.2 The Complementary Evaporation Principle

155 This principle, introduced formally by Bouchet (1963), is based on the common observation
156 that the actual evaporation E from a natural land surface under drying conditions and the
157 evaporation E_{pa} from a small wet surface area, located in the same environment and
158 surrounded by the drying surface, from which E is taking place, exhibit complementary
159 trends; thus as drying proceeds and less moisture is available, E will decrease while E_{pa} will
160 increase. The latter quantity is variously named the atmospheric evaporative demand or the
161 apparent potential evaporation. When ample moisture is available at the surface, both E and
162 E_{pa} assume the value of the potential evaporation, E_{po} , in accordance with Thornthwaite's
163 (1948) definition; under such conditions one has $E = E_{po} = E_{pa}$. Bouchet (1963) originally
164 assumed that as E becomes smaller than the potential evaporation E_{po} during drying, the

165 energy not used for E becomes available and raises the apparent potential evaporation by the
 166 same amount; thus, one has $(E_{po} - E) = (E_{pa} - E_{po})$, and this yields immediately his
 167 proposed relationship

$$168 \quad E = 2E_{po} - E_{pa} \quad (8)$$

169 This was later broadened in Brutsaert and Parlange (1998) by letting $(E_{po} - E)$ be
 170 proportional to $(E_{pa} - E_{po})$; this results in

$$171 \quad E = [(b+1)E_{po} - E_{pa}] / b \quad (9)$$

172 where b is a constant. Both (8) and (9) satisfy the condition that $E = E_{po}$ whenever
 173 $E_{pa} = E_{po}$, as it should. In a further generalization, with the imposition of three additional
 174 conditions, in Brutsaert (2015) $(E_{po} - E)$ could be represented by a cubic polynomial of
 175 $(E_{pa} - E_{po})$. This relationship can be expressed as

$$176 \quad E = \left(\frac{E_{po}}{E_{pa}} \right)^2 (2E_{pa} - E_{po}) \quad (10)$$

177 To apply (8), (9) or (10) it is necessary to estimate E_{pa} and E_{po} . As defined earlier, the
 178 atmospheric evaporative demand E_{pa} is the evaporation from a small moist surface area,
 179 located in the same environment and surrounded by the drying surface from which E is
 180 occurring. This definition indicates that it can be measured directly using a small pan (Kahler
 181 and Brutsaert, 2006; Brutsaert, 2006; 2013; Zhang et al., 2017); alternatively, as proposed in
 182 Brutsaert and Stricker (1979) with (8), and confirmed in subsequent studies, it can also be
 183 closely described by means of Penman's (1948, 1956) equation, with the variables measured
 184 under the ambient nonpotential conditions. This can be written as

185
$$E_{pa} = \frac{\Delta}{\Delta + \gamma} Q_{ne} + \frac{\gamma}{\gamma + \Delta} f_e(u_2)(e_1^* - e_1) \quad (11)$$

186 in which $\Delta \equiv de^* / dT$ is the slope of the saturation vapor pressure curve, γ is the
 187 psychrometric constant, and $Q_{ne} = (R_n - G) / L_e$ is the available energy expressed in
 188 evaporation units, with R_n the net radiation, G the heat flux into the ground (often neglected
 189 for daily averages), and L_e the latent heat of vaporization; the variable u_2 is the mean wind
 190 speed measured at a height z_2 above the ground, e_1 is the vapor pressure at a height z_1
 191 above the ground, and the asterisk means saturation. Zhang et al.(2017) and Liu et al.(2018)
 192 showed that at the daily time scale the implementation of (11) is fairly insensitive to the
 193 selected wind function $f_e(u_2)$, in the context of the complementary approach; thus, the wind
 194 function can be represented by *Penman's*[1948] simple empirical equation

195
$$f_e(u_2) = 0.26(1 + 0.54u_2) \quad (12)$$

196 The constants in this equation are for wind speeds (in $m s^{-1}$) and vapor pressures (in hPa)
 197 measured at 2 m above the ground and they produce the resulting second term on the right of
 198 (11) in $mm d^{-1}$.

199 The E_{po} term is more difficult to estimate. One reason is that it was originally conceived as
 200 potential evaporation. Thus, as defined by Thornthwaite (1948) the measurements needed in
 201 its estimation must be made under truly potential conditions, that is, with sufficient water
 202 present at the evaporating surface; these are never available when E is to be estimated under
 203 non-potential conditions. In the advection-aridity approach with (8) in Brutsaert and Stricker
 204 (1979), and other early implementations of the complementary approach, the E_{po} term was

205 assumed to be proportional to the equilibrium evaporation introduced by Slatyer and McIlroy
 206 (1961) as

$$207 \quad E_e = \frac{\Delta}{\Delta + \gamma} Q_{ne} \quad (13)$$

208 The proportionality constant was taken to be $\alpha_e = 1.26$, the standard value for potential
 209 conditions given by Priestley and Taylor (1972). In Brutsaert and Stricker (1979) it was
 210 assumed (and hoped) that $\alpha_e E_e$ would be sufficiently robust to provide a stable estimate of
 211 E_{po} under any conditions. However, subsequent calibration studies with better experimental
 212 data revealed that this is not the case and that the α_e parameter must be allowed to vary; this
 213 variation was shown to depend mostly on the aridity index $AI = E_{pa} / P$ (Liu et al. 2016;
 214 2018; Brutsaert et al., 2020). To avoid further confusion with the α_e parameter of Priestley
 215 and Taylor, henceforth the variable proportionality will be denoted β . Accordingly, after
 216 replacing E_{po} by βE_e , Equation (10) becomes finally

$$217 \quad \frac{E}{E_{pa}} = 2 \left(\frac{\beta E_e}{E_{pa}} \right)^2 - \left(\frac{\beta E_e}{E_{pa}} \right)^3 \quad (14)$$

218 in which E_e is defined in (13), and E_{pa} in (11). For further analysis (14) can be written more
 219 concisely as

$$220 \quad y = 2x^2 - x^3 \quad (15)$$

221 in which $y = (E / E_{pa})$ and $x = (\beta E_e / E_{pa})$. The estimation of the variable parameter β and
 222 of its functional form is the main objective of this paper; this is treated next.

223 2.3 Blending of Evaporation/Precipitation Ratio with Complementary Function

224 Elimination of (E/E_{pa}) between (14) (or (15)) and (7) in which $E_{\max} = E_{pa}$, yields their
 225 combination as a cubic equation, to wit

$$226 \quad x^3 - 2x^2 + z = 0 \quad (16)$$

227 in which $z = F(P/E_{pa}) = 1 + (P/E_{pa}) - [1 + (P/E_{pa})^w]^{1/w}$. The appropriate solution of (16)
 228 can be written as (Oldham, Myland and Spanier, 2009)

$$229 \quad x = \frac{2}{\sqrt{3}} \sqrt{-p} \sin \left(\frac{1}{3} \sin^{-1} \left(\frac{3\sqrt{3}}{2(\sqrt{-p})^3} q \right) \right) + \frac{2}{3} \quad (17)$$

230 where $p = -4/3$ and $q = (-16/27 + z)$. This yields the parameter β in terms of E_e , E_{pa}
 231 and P , as follows

$$232 \quad \beta = \left(\frac{E_{pa}}{E_e} \right) \left[\frac{4}{3} \sin \left(\frac{1}{3} \sin^{-1} \left(\frac{27}{16} z - 1 \right) \right) + \frac{2}{3} \right] \quad (18)$$

233 This can also be written concisely as

$$234 \quad \beta = \Psi^{-1} \left[\frac{4}{3} \sin \left(\frac{1}{3} \sin^{-1} \left(\frac{27}{16} F(\Phi) - 1.0 \right) \right) + \frac{2}{3} \right] \quad (19)$$

235 where $\Psi = E_e/E_{pa}$, $\Phi = P/E_{pa}$, and $F(\Phi) = 1 + \Phi - [1 + \Phi^w]^{1/w}$. The optimal value of the
 236 parameter w will be determined in Section 4.1.1. The analogous relationship for the linear
 237 complementary relationship (9) is shown in Appendix 1.

238

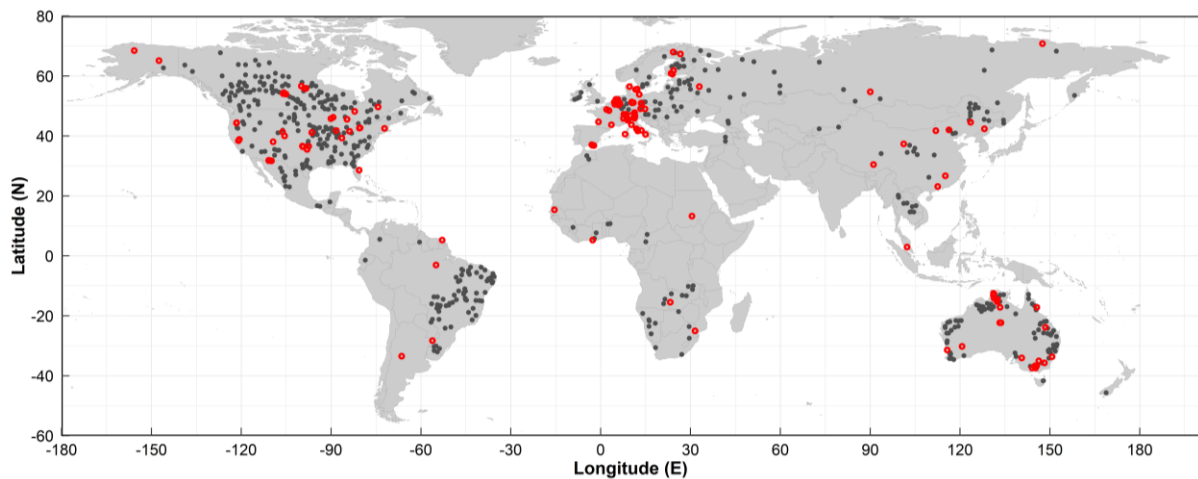
239

240 **3. Data Description**

241 This study used the data obtained from global catchment water balance data and eddy
242 covariance flux measurements. The global catchment water balance data were used for
243 method development, while the eddy covariance flux data were used for method application
244 and validation.

245 3.1. Data for method development

246 The global catchment water balance data include reliable mean annual streamflow and
247 precipitation data from 524 catchments located in different geographic regions of the world
248 (Figure 1).



249 **Figure 1.** Location map of the global catchments (black dots) (n=524) where the annual
250 evaporation was measured with the water budget equation; these values were used to develop
251 the proposed method. Also shown is the spatial distribution of the global flux stations (red
252 circles) (n=156) used in the validation process.
253

254

255 All the 524 selected catchments are identified as unregulated with minimal effect of dams or
256 reservoirs. The streamflow data from these catchments for the period of 2001-2013 were
257 obtained from (i) the Global Runoff Data Centre
258 (http://www.bafg.de/GRDC/EN/Home/homepage_node); (ii) unregulated Australian
259 catchments (Zhang et al., 2013); (iii) the Model Parameter Estimation Experiment (MOPEX)
260 across the United States (<http://www.nws.noaa.gov/oh/mopex/index.html>); and (iv) runoff

261 data gathered by the Chinese Academy of Sciences. Precipitation data were obtained from the
262 global cover MSWEP rainfall dataset (Beck et al. 2017; Sun et al. 2018). For each of these
263 catchments, the mean annual precipitation for 2001-2013 was calculated with an area
264 weighted averaging technique. The mean annual values of evaporation from these catchments
265 were calculated based on the water balance equation by neglecting changes in catchment
266 water storage.

267 Daily values of meteorological variables such as air temperature, humidity, and wind speed
268 were obtained from the CRU-NECP dataset (version 7, New et al., 1999). This dataset was
269 produced by merging observed mean monthly data of the Climate Research Unit (CRU) at
270 the University of East Anglia, with NOAA's high temporal resolution NCEP reanalysis data
271 at a spatial resolution of 0.5° . The mean annual pressure was used to represent the
272 atmospheric pressure and the wind speed at 10 m above the ground was converted to a height
273 of 2 m by multiplying it by $(2/10)^{1/7}$ (Brutsaert, 2005). Daily net radiation values were
274 obtained from the Clouds and the Earth's Radiant Energy System (CERES) SYN1deg-Day
275 dataset with spatial resolution of 1.0° (Wielicki et al., 1996). A local averaging method was
276 used to resample the net radiation data to 0.5° to achieve the resolution of the other
277 atmospheric inputs. The ground heat flux was considered negligible on a daily basis.

278 The above daily meteorological data were then used to calculate E_e and E_{pa} by means of
279 (13) and (11) over the period of 2001-13 at a spatial resolution of 0.5° . The catchment mean
280 annual values of E_e and E_{pa} were calculated with an area weighted averaging method, in the
281 same way as mean annual precipitation.

282

283 3.2 Data for method application and validation

284 For the purpose of more detailed application and independent validation of the proposed
285 method, a selection was made of 156 eddy covariance flux stations from the global
286 FLUXNET2015 dataset (<http://fluxnet.fluxdata.org/>), with the criterion that each station had
287 at least one full year of complete and continuous daily data. The data from these 156
288 FLUXNET stations comprise evaporation measurements using the eddy covariance technique,
289 beside measurements of the standard near surface atmospheric variables. At all stations
290 energy budget closure was achieved by adjusting the eddy covariance flux measurements as
291 suggested by Twine et al. (2000) and others. The β value of each station was obtained by
292 solving equation (14) at the mean annual time scale, with annual averages of daily values.
293 Among the 156 flux stations, 28 stations were selected for estimating daily evaporation rates
294 and details of these stations are listed in Table 1. These 28 stations were selected so they
295 would represent as wide a geographic and climatic distribution as possible.

296 Table 1. Details of flux stations used for estimating daily evaporation rates in the study.

Station ID	Lat.	Lon.	IGBP	Period of Record
AU-DaS	-14.1593	131.3881	GRA	2008-2014
AU-Gin	-31.3764	115.7138	WSA	2011-2014
AU-GWW	-30.1913	120.6541	SAV	2013-2014
AU-How	-12.4943	131.53	WSA	2003-2014
AU-Stp	17.1507	133.3502	GRA	2008-2014
AU-Tum	-35.6566	148.1517	EBF	2001-2014
BE-Vie	50.30493	5.99812	MF	1996-2014
BR-Sa3	-3.01803	-54.97144	EBF	2000-2004
CA-Gro	48.2167	-82.1556	MF	2003-2014
CN-Du3	42.0551	116.2809	GRA	2009-2010
DE-Geb	51.09973	10.91463	CRO	2001-2014
DE-Kli	50.89306	13.52238	CRO	2004-2014
DE-SfN	47.80639	11.3275	WET	2012-2014
DK-Eng	55.69053	12.19175	GRA	2005-2008
ES-Amo	36.83361	-2.25232	OSH	2007-2012
ES-LJu	36.92659	-2.75212	OSH	2004-2013
FI-Let	60.64183	23.95952	ENF	2009-2012
FI-Lom	67.99724	24.20918	WET	2007-2009
FR-LBr	44.71711	-0.7693	ENF	1996-2008
GH-Ank	5.26854	-2.69421	EBF	2011-2014
IT-BCi	40.52375	14.95744	CRO	2009-2011
IT-Noe	40.60618	8.11529	CSH	2004-2014

IT-Tor	45.84444	7.57806	GRA	2008-2014
MY-PSO	2.9730	102.3062	EBF	2003-2009
RU-Fyo	56.46153	32.92208	ENF	1998-2014
US-Blo	38.8953	-120.6328	ENF	1997-2007
US-MMS	39.3232	-86.4131	DBF	1999-2014
US-Syv	46.2420	-89.3477	MF	2001-2008

297

298 4. Results and Discussion

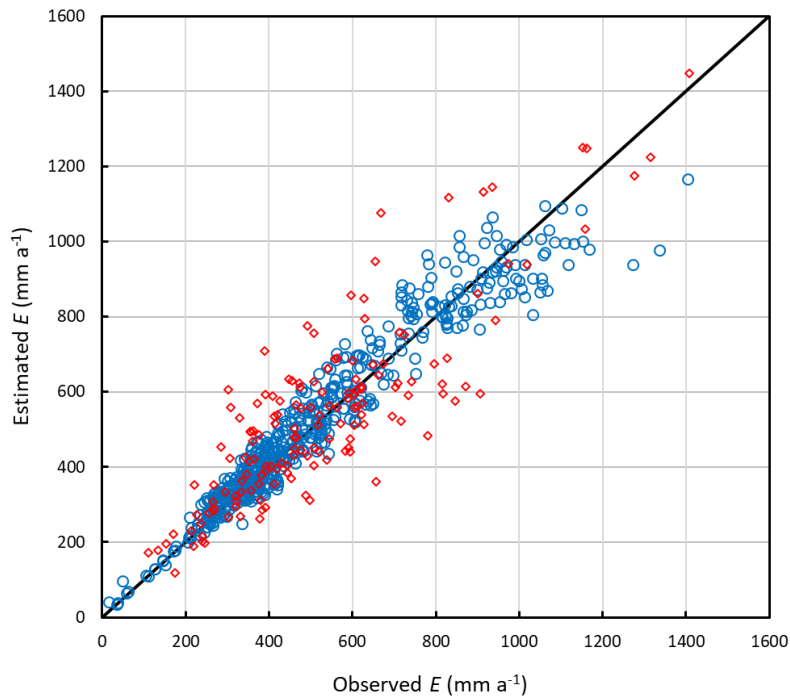
299 4.1. Method development

300 4.1.1. Estimation of Tixeront-Fu parameter w

301 The Tixeront-Fu parameter w was determined by calibrating (7) against the water balance
302 estimates of evaporation from the 524 selected catchments with $E_{\max} = E_{pa}$. The calibration
303 was done by trial and error, adjusting w until the slope through the origin was exactly 1.0
304 between observed and estimated mean annual evaporation (Figure 2). The Nash-Sutcliffe
305 efficiency (NSE) is 0.93, the correlation coefficient is 0.96 and the bias 2.12%, indicating a
306 good model calibration. The value of the optimized w is 2.41; this is close to the reported
307 value of 2.53 by Zhang et al. (2004) and 2.50 by Xu et al. (2013). Also shown in Figure 2 are
308 the mean annual values of evaporation estimated using (7) with the optimized $w = 2.41$ for
309 the 156 global flux sites. The NSE is 0.71 and the correlation coefficient is 0.83 with a bias of
310 2.15%. These results indicate that equation (7) with the optimized $w = 2.41$ can accurately
311 predict mean annual evaporation when compared with global catchment water balance data
312 and flux measurements.

313 It can be noted in Figure 2 that equation (7) provided more accurate estimates of mean annual
314 evaporation for the selected catchments than the flux stations. This may be due to the fact that
315 the catchment water balance estimates of evaporation are averaged over the catchments for a
316 period of 12 years, while the flux stations represent point measurements and the record

317 lengths are also shorter. This difference in performance for the two sets of data will also be
318 seen again in the other figures which follow in this paper.



319

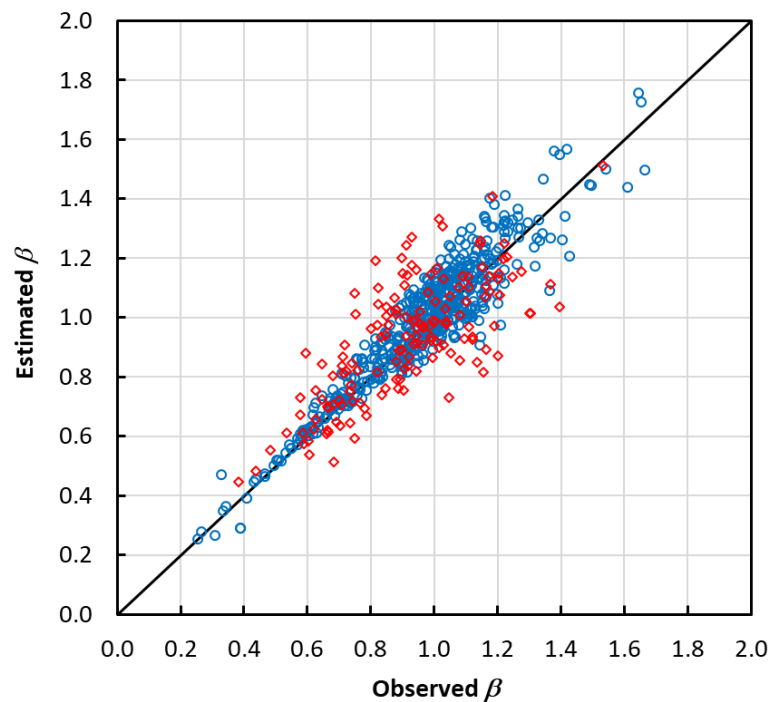
320 **Figure 2.** Comparison between the mean annual evaporation estimated using (7) with optimal
321 parameter $w = 2.41$ against the water balance estimates for 524 selected catchments (blue
322 open circles). Also shown are the mean annual evaporation estimates using (7) with optimal
323 parameter $w = 2.41$ against observed mean annual evaporation from 156 global flux stations
324 (red diamonds).

325

326 4.1.2. Estimation of the model parameter β

327 The main part of this study is to develop a prediction method for the model parameter β from
328 climatic variables, i.e. E_e and E_{pa} in the absence of information on E . For each catchment,
329 the parameter β was predicted from (19) with the optimized $w = 2.41$. These predicted
330 parameter β values can be compared with “observed” β values for the 524 selected
331 catchments in Figure 3. The “observed” parameter β values were obtained by inverting
332 equation (14) numerically with the value of mean annual evaporation calculated from the

333 water balance method and E_e and E_{pa} determined with (13) and (11). The Nash-Sutcliffe
 334 efficiency (NSE) is 0.85, the correlation coefficient is 0.92 and the bias 2.11%. The
 335 performance of (19) in predicting the parameter β was also assessed by comparing the
 336 predicted and “observed” β values for the flux stations (Figure 3). Similarly, the observed
 337 β values for the flux stations were obtained with (14) from the measured mean annual
 338 evaporation values using the eddy covariance technique. The Nash-Sutcliffe efficiency (NSE)
 339 is 0.49, the correlation coefficient is 0.67 and the bias 1.45%, indicating a reasonably
 340 accurate prediction of the parameter β for the flux stations.

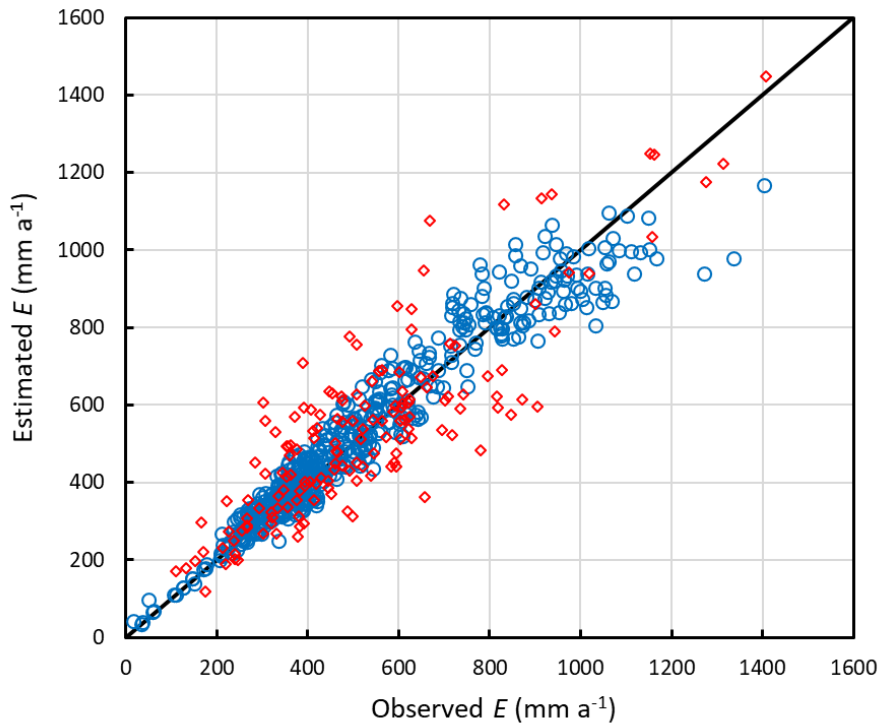


341
 342 **Figure 3.** Comparison of the calculated β values by equation (19) against “observed” values
 343 by inverting (14) for the 524 catchments shown in Figure 1 (blue circles). Also shown are the
 344 corresponding β values from the data at the 156 flux stations (red diamonds).

345

346 4.1.3. Estimation of mean annual evaporation

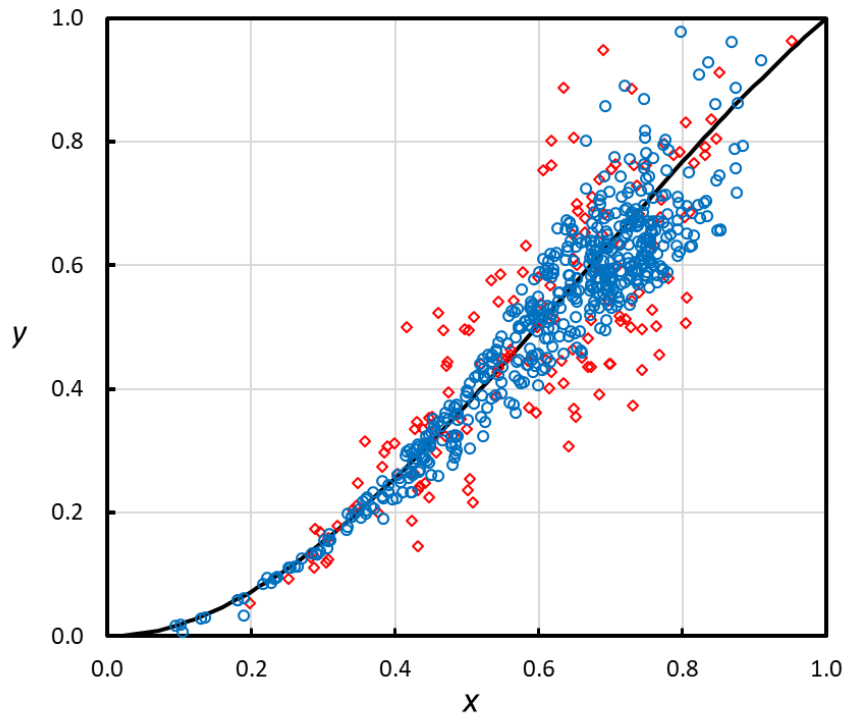
347 The values of mean annual evaporation estimated using (14) with the model parameter β
348 predicted using (19) are compared against the estimates made by the water balance of the 524
349 selected catchments in Figure 4. The Nash-Sutcliffe efficiency (NSE) is 0.93, the correlation
350 coefficient is 0.96 and the bias is -2.08%. These results indicate a good fit between the
351 estimated and observed values. Also shown in Figure 4 is a comparison of the mean annual
352 values of evaporation values for the 156 global flux sites estimated the same way. The NSE is
353 0.71 and the correlation coefficient is 0.83 with a bias of 1.88%. Both the water balance
354 estimates of mean annual evaporation and flux measurements support the validity of the
355 complementary relationship in (14) (Figure 5) and show that actual evaporation and apparent
356 potential evaporation exhibit a strong asymmetrical complementary relationship (Figure 6).
357 These results indicate that the complementary principle-based approach with the parameter
358 β determined by (19) can accurately predict mean annual evaporation. As illustrated in
359 Figures 2 and 4, both equations (7) and (14) prove to be accurate for estimating mean annual
360 evaporation. However, it should be noted that equation (7) needs only one constant parameter
361 w , while the complementary principle-based approach with (14) requires a variable parameter
362 β which is a function of two dimensionless quantities as indicated in (19). But the
363 disadvantage of (7) is that it can only be applied at annual or larger time scales.



364

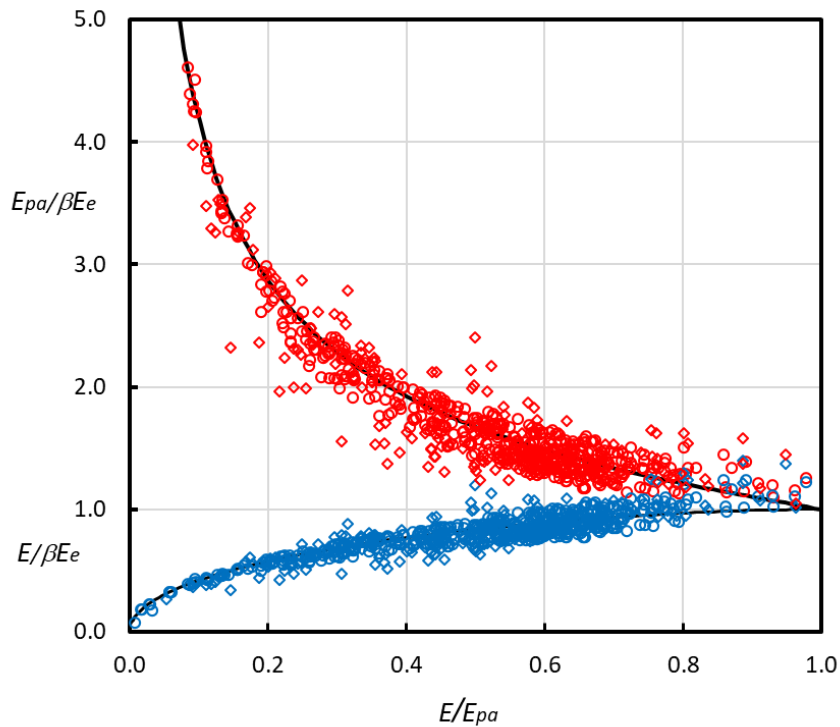
365 **Figure 4.** Comparison between mean annual evaporation estimated using (14) with parameter
 366 β determined by (19) against water balance estimates for 524 selected catchments (blue open
 367 circles). Also shown are the mean annual evaporation values estimated the same way, against
 368 the observed mean annual evaporation for the 156 global flux stations (red diamonds).

369



370

371 Figure 5. Relationship between scaled evaporation $y = (E / E_{pa})$ and scaled reference
 372 evaporation $x = (\beta E_e / E_{pa})$. The catchment water balance data are shown as blue circles (n
 373 = 524) and the global flux measurements as red diamonds ($n = 156$). The theoretical
 374 complementary relationship (14) or (15) is represented by the curve.



375
 376 Figure 6. Illustration of the complementary relationship between the actual evaporation E
 377 and the atmospheric evaporative demand (or apparent potential evaporation) E_{pa} , relative to
 378 βE_e , for varying conditions of moisture availability, as expressed by their ratio E / E_{pa} . The
 379 open circles represent the water balance data ($n = 524$) and the diamonds represent global
 380 flux measurements ($n = 156$). The curves show the theoretical relationship (14) or (15), as
 381 (y / x) and $(1 / x)$ against y .

382

383 4.2. Prediction of daily evaporation

384 4.2.1. Proposed procedure

385 Equation (19) is the result of a fusion of the evaporation/precipitation ratio with the
386 complementary principle function and it allows the direct prediction of the parameter β
387 without the need of evaporation measurements for its calibration. The results shown in
388 Figure 4 indicate that the complementary principle-based approach can provide accurate
389 estimates of mean annual evaporation from routine meteorological data with the predicted
390 parameter β ; from equation (19). Here we now make the assumption that the mean annual β
391 relationship (i.e. equation (19)) can also be used at shorter time scales, such as a day. To test
392 this assumption, the complementary principle equation (14) can now be used to estimate daily
393 values of evaporation from the 28 selected flux stations under different climatic conditions
394 listed in Table 1. The model parameter β for each flux station was estimated with equation
395 (19) and assumed constant through the year. The estimated daily evaporation rates using (14)
396 were compared against the flux measurements, and the resulting statistics are listed in Table 2.
397 The Nash-Sutcliffe efficiency (NSE) is larger than 0.50 in 66% of the flux stations, the
398 correlation coefficient is larger than 0.83 in 27 out of the 28 flux stations. The slope of the
399 daily evaporation plots through the origin is close to 1.0 for most stations. As expected, flux
400 stations under dry climatic conditions (e.g. aridity index larger than 3) showed less accurate
401 results as compared to the more humid flux stations. However, this may not necessarily be a
402 reflection of the performance of the model itself. As a further illustration, some results of the
403 daily evaporation estimates are also shown in Figure 7 for a subset of the flux stations (n=12);
404 these graphs reinforce the good agreement shown in Table 2. Figure 7 also illustrates why a
405 low correlation may not necessarily reflect poorly on the performance of the model. For
406 instance, graph (a) (AU-Gin in Table 2) and graph (k) (RU-Fyo in Table 2) display a similar
407 spread of the data, yet in Table 2 the former has a correlation coefficient r of 0.89 and a slope
408 of 0.82, whereas for the latter these values are 0.95 and 1.03. The main reason for this

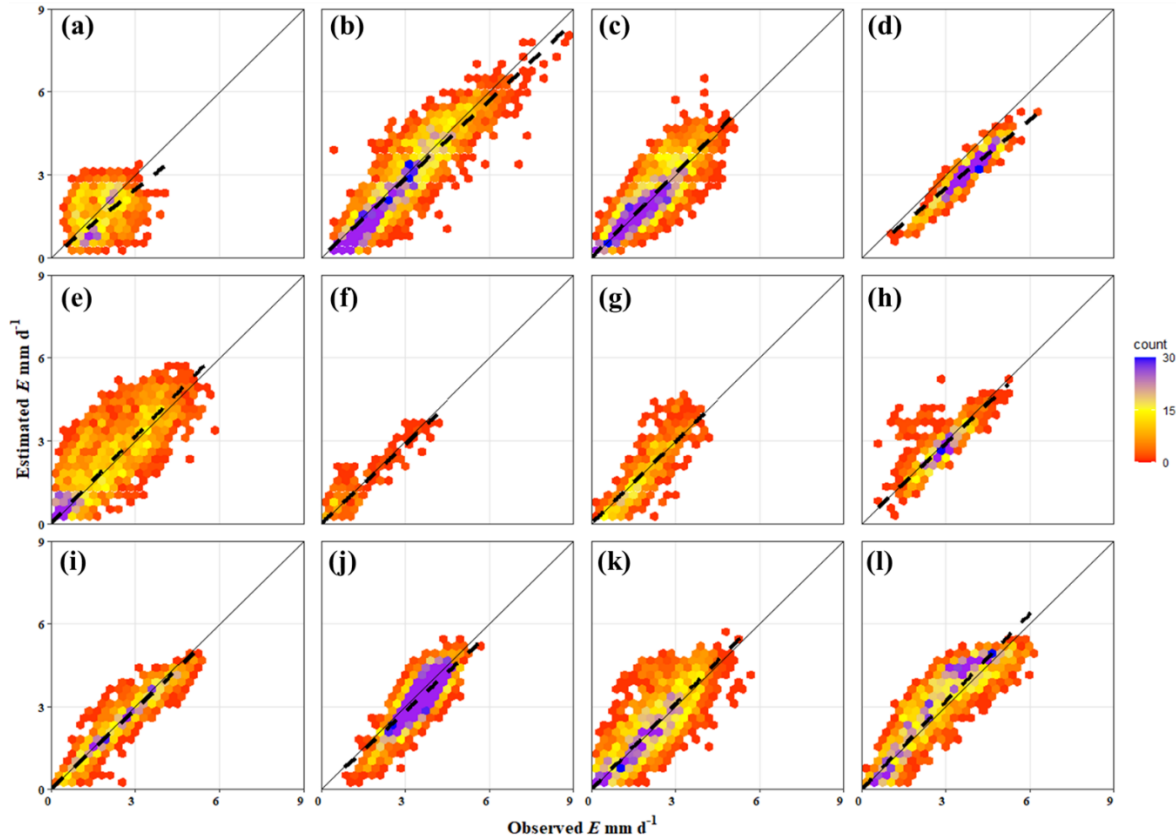
409 difference is that the drier Australian site has a narrower range of E values than the more
 410 humid Russian site.

411

412 Table 2. Statistics of daily evaporation estimated with predicted parameter β from Eq. (19) against
 413 eddy covariance measurements from selected global flux stations.

Station ID	AI	β	Slope	r	NSE	Bias (%)	RMSE (mm/d)
AU-DaS	1.40	0.95	1.02	0.98	0.63	-6.7	0.7
AU-Gin	3.10	0.71	0.82	0.89	-0.44	12.1	0.86
AU-GWW	6.18	0.61	0.74	0.88	-0.35	19.5	0.53
AU-How	1.05	0.98	0.95	0.97	0.34	-0.10	0.88
AU-Stp	3.01	0.91	0.91	0.91	0.03	-18.4	0.88
AU-Tum	1.20	1.07	0.95	0.98	0.83	7.5	0.68
BE-Vie	1.13	0.97	1.01	0.97	0.74	-3.3	0.61
BR-Sa3	0.83	1.02	0.91	0.99	0.70	11.60	0.47
CA-Gro	1.37	1.11	1.05	0.94	0.65	-11.7	0.89
CN-Du3	2.91	1.14	0.95	0.95	0.78	-1.9	0.45
DE-Geb	1.53	1.14	0.91	0.94	0.57	-0.4	0.8
DE-Kli	0.92	1.29	1.08	0.95	0.59	-13.1	0.89
DE-SfN	1.06	0.91	0.94	0.99	0.88	7.8	0.49
DK-Eng	1.21	1.16	0.99	0.96	0.71	3.7	0.6
ES-Amo	6.08	0.57	0.80	0.63	-1.30	-27	0.61
ES-LJu	3.14	0.78	1.13	0.89	0.14	-23.9	0.71
FI-Let	1.57	0.90	0.97	0.96	0.75	0.4	0.52
FI-Lom	1.14	1.14	1.04	0.99	0.94	-2.1	0.26
FR-LBr	1.23	1.00	0.97	0.95	0.53	0.9	0.89
GH-Ank	0.76	0.93	0.96	0.98	0.48	2.2	0.56
IT-BCi	0.87	1.13	0.98	0.93	0.32	-3.4	1.26
IT-Noe	2.60	0.67	1.06	0.83	-0.40	-10.6	0.79
IT-Tor	0.73	1.19	0.97	0.99	0.87	18.4	0.79
MY-PSO	0.90	0.92	0.94	0.99	0.67	5.2	1.06
RU-Fyo	1.21	0.94	1.03	0.95	0.68	-7.9	0.69
US-Blo	1.09	1.03	1.06	0.98	0.78	-17.5	1.24
US-MMS	1.16	1.09	0.96	0.97	0.75	0.1	0.72
US-Syv	1.23	1.06	0.92	0.95	0.69	0.1	0.72

414



415

416 **Figure 7.** Comparison of daily evaporation estimated using equation (14) with model
 417 parameter β obtained from equation (19) against the eddy covariance measurements at (a)
 418 Gingin (Australia), (b) Tumbarumba (Australia), (c) Vielsalm (Belgium), (d) Santarem
 419 (Brazil), (e) Ontario (Canada), (f) Duolun (China), (g) Enghave (Denmark), (h) Ankasa
 420 (Ghana), (i) Torgnon (Italy), (j) Pasoh Forest Reserve (Malaysia), (k) Fyodorovskoye
 421 (Russia), (l) Blodgett Forest (USA). Filling color of the bins depends on the number of points
 422 (i.e., counts) in each bin.

423

424 5. Conclusions

425 The method for estimating evaporation based on the Schreiber-Oldekop hypothesis, also
 426 commonly known as the Budyko framework, relates the evaporation precipitation ratio with
 427 aridity index. In this study, an equivalent and mutually convertible form of the relationship
 428 (i.e. the Tixeront-Fu equation) with E_{\max} estimated using the Penman equation as repeating
 429 variable was tested against observed evaporation from global datasets of catchment water

430 balance and eddy covariance flux measurements and was found to yield excellent agreement
431 at the mean annual time scale, with an optimized parameter $w = 2.41$. This value is close to w
432 values obtained in previous studies. By selecting the atmospheric evaporative demand, E_{pa}
433 to represent the maximum possible evaporation E_{max} , the evaporation precipitation ratio and
434 the complementary relationship could be blended into an analytical equation to predict the
435 parameter β of the latter; this made the generalized complementary approach essentially
436 calibration-free. With predicted parameter values from the analytical equation, the
437 complementary principle approach provided accurate estimates of evaporation not only at the
438 mean annual time scale, but also at shorter such as daily time scales. One of the main
439 strengths of this approach is that it allows the prediction of daily evaporation using only
440 routine meteorological inputs including air temperature, humidity, wind speed, net radiation,
441 and long-term average precipitation.

442

443 **Acknowledgments.** This study used eddy covariance data acquired and shared by the
444 FLUXNET community, including these networks: AmeriFlux, AfriFlux, AsiaFlux,
445 CarboAfrica, CarboEuropeIP, CarboItaly, CarboMont, ChinaFlux, Fluxnet-Canada,
446 GreenGrass, ICOS, KoFlux, LBA, NECC, OzFlux-TERN, TCOS-Siberia, and TERENO and
447 USCCC. The FLUXNET EC data processing and harmonization was carried out by the ICOS
448 Ecosystem Thematic Center, AmeriFlux Management Project, and Fluxdata project of
449 FLUXNET, with the support of CDIAC, and the OzFlux, ChinaFlux, and AsiaFlux offices.
450 MTCI data are provided courtesy of the NERC Earth Observation Data Centre (NEODC),
451 ESA who provided the original data, and Astrium GEO-Information Services who processed
452 these data. The authors wish to thank Lei Cheng for providing the global catchment data and
453 Shujing Qin, Linyuan Ye, and Rong Gan for helping with daily evaporation calculations.

454 **References**

- 455 Andréassian, V., Mander, Ü., Pae, T. (2016). The Budyko hypothesis before Budyko: The
456 hydrological legacy of Evald Oldekop. *J. Hydrol.*, 535, 386–391.
457 <http://dx.doi.org/10.1016/j.jhydrol.2016.02.002>
- 458 Andréassian, V and Sari, T. (2019). Technical Note: On the puzzling similarity of two water balance
459 formulas – Turc–Mezentsev vs. Tixeront–Fu. *Hydrol. Earth Syst. Sci.*, 23, 2339–2350,
460 <https://doi.org/10.5194/hess-23-2339-2019>
- 461 Beck, H. E., van Dijk, A. I. J. M., Levizzani, V., Schellekens, J., Miralles, D. G., Martens, B. and de
462 Roo, A. (2017). MSWEP: 3-hourly 0.258 global gridded precipitation (1979–2015) by merging gauge,
463 satellite, and reanalysis data. *Hydrol. Earth Syst. Sci.*, 21, 589–615, [https://doi.org/10.5194/hess-21-](https://doi.org/10.5194/hess-21-589-2017)
464 [589-2017](https://doi.org/10.5194/hess-21-589-2017).
- 465 Bouchet, R. (1963). Evapotranspiration réelle et potentielle, signification climatique, *IAHS Publ.*, 62,
466 134–142 (in French).
- 467 Brutsaert, W. (1982). *Evaporation Into the Atmosphere: Theory, History, and Applications*, pp. 299,
468 Kluwer Acad., Dordrecht, Netherlands.
- 469 Brutsaert, W. (2005). *Hydrology: An Introduction*, 605 pp., Cambridge Univ. Press, N. Y.
- 470 Brutsaert, W. (2006). Indications of increasing land surface evaporation during the second half of the
471 20th century, *Geophys. Res. Lett.*, 33, L20403, doi:10.1029/2006GL027532.
- 472 Brutsaert, W. (2013). Use of pan evaporation to estimate terrestrial evaporation trends: The case of
473 the Tibetan Plateau. *Water Resour. Res.*, 49, 3054–3058, <https://doi.org/10.1002/wrcr.20247>.
- 474 Brutsaert, W. (2015). A generalized complementary principle with physical constraints for land-
475 surface evaporation, *Water Resour. Res.*, 51, 8087–8093, doi:10.1002/2015WR017720.
- 476 Brutsaert, W., Li, W., Takahashi, A., Hiyama, T., Zhang, L., and Liu, W. Z. (2017). Nonlinear
477 advection-aridity method for landscape evaporation and its application during the growing season in
478 the southern Loess Plateau of the Yellow River basin, *Water Resour. Res.*, 53,
479 doi:10.1002/2016WR019472.
- 480 Brutsaert, W., and Stricker, H. (1979). An advection-aridity approach to estimate actual regional
481 evapotranspiration, *Water Resour. Res.*, 15, 443–450, doi:10.1029/WR015i002p00443.
- 482 Brutsaert, W., and Parlange, M. B. (1998). Hydrologic cycle explains the evaporation paradox, *Nature*,
483 396(5), 300.
- 484 Brutsaert, W., Cheng, L., and Zhang, L. (2020). Spatial Distribution of Global Landscape Evaporation
485 in the Early Twenty First Century by Means of a Generalized Complementary Approach. *Journal of*
486 *Hydrometeorology*, <https://doi.org/10.1175/JHM-D-19-0208.1>
- 487 Budyko, M. I. (1958). The heat balance of the Earth’s surface, *Natl. Weather Serv., U.S. Dep. of*
488 *Commer., Washington, D. C.*
- 489 Budyko, M. I. (1974). *Climate and Life*, 508 pp., Academic, San Diego, Calif.
- 490 Crago, R. D., and Qualls, R. J. (2018). Evaluation of the generalized and rescaled complementary
491 evaporation relationships. *Water Resources Research*, 54, 8086–8102. [https://doi.org/10.1029/](https://doi.org/10.1029/2018WR023401)
492 [2018WR023401](https://doi.org/10.1029/2018WR023401)

- 493 Crago, R., Szilagyi, J., Qualls, R. and Huntington, J. (2016). Rescaling the complementary
494 relationship for land surface evaporation, *Water Resour. Res.*, 52, 8461–8471.
495 doi:10.1002/2016WR019753.
- 496 Fu, B. P. (1981). On the calculation of the evaporation from land surface (in Chinese), *Sci. Atmos.*
497 *Sin.*, 5, 23– 31.
- 498 Hobbins, M. T., J. A. Ramírez, and Brown, T. C. (2001). The complementary relationship in
499 estimation of regional evapotranspiration: An enhanced Advection-Aridity Model, *Water Resour. Res.*,
500 37(5), 1389–1403, doi:10.1029/2000WR900359.
- 501 Kahler, D. M., and Brutsaert, W. (2006). Complementary relationship between daily evaporation in
502 the environment and pan evaporation. *Water Resour. Res.*, 42, W05413,
503 <https://doi.org/10.1029/2005WR004541>.
- 504 Lemeur, R., and Zhang, L. (1990). Evaluation of three evapotranspiration models in terms of their
505 applicability for an arid region, *J. Hydrol.*, 114(3), 395–411, doi:10.1016/0022-1694(90)90067-8.
- 506 Lhomme, J-P and Moussa, R. (2016). Matching the Budyko functions with the complementary
507 evaporation relationship: consequences for the drying power of the air and the Priestley-Taylor
508 coefficient. *Hydrol. Earth Syst. Sci.*, 20, 4857–4865, doi:10.5194/hess-20-4857-2016.
- 509 Li, D., Cong, ZT, Zhang, L, and Wood, E (2013). Vegetation control on water and energy balance
510 within the Budyko framework. *Water Resour. Res.* 49, 1–8, doi:10.1002/wrcr.20107
- 511 Liu, X., C. Liu, and Brutsaert, W. (2016). Regional evaporation estimates in the eastern monsoon
512 region of China: Assessment of a nonlinear formulation of the complementary principle. *Water*
513 *Resour. Res.*, 52, 9511–9521, <https://doi.org/10.1002/2016WR019340>.
- 514 Liu, X., C. Liu, and Brutsaert, W. (2018). Investigation of a generalized nonlinear form of the
515 complementary principle for evaporation estimation. *J. Geophys. Res. Atmos.*, 123, 3933–3942,
516 <https://doi.org/10.1002/2017JD028035>.
- 517 McMahon, T. A., Peel, M. C., Lowe, L., Srikanthan, R and McVicar, T.R. (2013). Estimating actual,
518 potential, reference crop and pan evaporation using standard meteorological data: A pragmatic
519 synthesis, *Hydrol. Earth Syst. Sci.*, 17(4), 1331–1363, doi:10.5194/hess-17-1331-2013.
- 520 Morton, F. I. (1983). Operational estimates of areal evapotranspiration and their significance to the
521 science and practice of hydrology, *J. Hydrol.*, 66, 1–76.
- 522 New, M., Hulme, M, and Jones, P. (1999). Representing twentieth century space–time climate
523 variability. Part I: Development of a 1961–90 mean monthly terrestrial climatology. *J. Climate*, 12,
524 829–856, [https://doi.org/10.1175/1520-0442\(1999\)012,0829: RTCSTC.2.0.CO;2](https://doi.org/10.1175/1520-0442(1999)012<0829: RTCSTC.2.0.CO;2).
- 525 Oldham, K, Myland, J, and Spanier, j. (2009). *An Atlas of Functions with Equator, the Atlas Unction*
526 *Calculator*, Second Edition. Springer Science+Business Media, LLC, 748pp.
- 527 Oldekop, E. (1911). On evaporation from the surface of river basins. (In Russian: Ob Isparenii s
528 Poverkhnosti Rechnykh Basseinov), (With abstract in German, p. 201-209). Collection of the Works
529 of Students of the Meteorological Observatory. University of Tartu-Jurjew-Dorpat, Tartu, Estonia,
530 209pp.
- 531 Parlange, M.B. and Katul, G.G. (1992). An advection-aridity evaporation model, *Water Resour. Res.*,
532 28, 127-132, 1992.
- 533 Penck, A. (1896). Untersuchungen über Verdunstung und Abfluss von grösseren Landflächen. *Geogr.*
534 *Abh. Wien*, 5 (5), 10-29.

- 535 Penman, H. L. (1948). Natural evaporation from open water, bare soil, and grass, *Proc. R. Soc. A*, 193,
536 120–146.
- 537 Penman, H.L. (1956). Evaporation an Introductory Survey. *Netherlands Journal of Agricultural*
538 *Science*, 4, 9-29.
- 539 Priestley, C. H. B., and Taylor, R. J. (1972). On the assessment of the surface heat flux and
540 evaporation using large-scale parameters, *Mon. Weather Rev.*, 100, 81–92.
- 541 Schreiber, P. (1904). Über die Beziehungen zwischen dem Niederschlag und der Wasserführung der
542 Flüsse in Mitteleuropa. *Meteorol. Zeitsch.*, 21, 441-452.
- 543 Slatyer, R. O. and McIlroy, I. C. (1961). *Practical Microclimatology*, CSIRO, Melbourne, Victoria,
544 Australia, 310 pp.
- 545 Sposito, G. (2017). Understanding the Budyko equation. *Water*, 9 (4), 236, doi:10.3390/w9040236
- 546 Stigler, S. M. (1980). Stigler’s law of eponymy. *Trans. New York Acad. Sci.*, 39, 147–157. doi:
547 10.1111/j.2164-0947.1980.tb02775.
- 548 Sun, Q., Miao, C., Duan, Q., Ashouri, H., Sorooshian, S. and Hsu, K.-L. (2018). A review of global
549 precipitation data sets: Data sources, estimation, and intercomparisons. *Rev. Geophys.*, 56, 79–107,
550 <https://doi.org/10.1002/2017RG000574>.
- 551 Thornthwaite, C. W. (1948). An approach toward a rational classification of climate. *Geogr. Rev.*, 38,
552 55–94. <https://doi.org/10.2307/210739>.
- 553 Tixeront, J. (1964). *Prévision des apports des cours d’eau (Prediction of streamflow)*, IAHS
554 Publication 63: General Assembly of Berkeley. IAHS, Gentbrugge, pp. 118–126.
- 555 Twine, T. E., and Coauthors, (2000). Correcting eddy-covariance flux underestimates over a grassland.
556 *Agric. For. Meteor.*, 103, 279–300, [https://doi.org/10.1016/S0168-1923\(00\)00123-4](https://doi.org/10.1016/S0168-1923(00)00123-4).
- 557 Ule, W. (1903). Niederschlag und Abfluss in Mitteleuropa. *Forsch. Deutsche Volks- u. Landesk.*, 14
558 (5), 24-39.
- 559 Wang, C., Wang, S., Fu, B.J., and Zhang, L. (2016). Advances in hydrological modelling with the
560 Budyko framework: A review. *Progress in Physical Geography*, 1-22.
561 doi:10.1177/0309133315620997.
- 562 Wang, K., and Dickinson, R. E. (2012). A review of global terrestrial evapotranspiration: Observation,
563 modeling, climatology, and climatic variability. *Rev. Geophys.*, 50, RG2005,
564 <https://doi.org/10.1029/2011RG000373>.
- 565 Wielicki, B. A., Barkstrom, B. R., Harrison, E. F., Lee, R. B., Smith, G. L. and Cooper, J. E. (1996).
566 Clouds and the Earth’s Radiant Energy System (CERES): An Earth observing system experiment.
567 *Bull. Amer. Meteor. Soc.*, 77, 853–868, [https://doi.org/10.1175/1520-0477\(1996\)077,0853:CATERE.2.0.CO;2](https://doi.org/10.1175/1520-0477(1996)077,0853:CATERE.2.0.CO;2).
- 569 Xu, X.L., Liu, W., Scanlon, B.R., Zhang, L., and Pan, M. (2013). Local and global factors controlling
570 water-energy balances within the Budyko framework. *Geophysical Research Letters*. Vol, 40, 6123-
571 6129, doi: 10.1002/2013GL058324.
- 572 Yang, D., Sun, F., Liu, Z., Cong, Z., and Lei, Z. (2006). Interpreting the complementary relationship
573 in non-humid environments based on the Budyko and Penman hypotheses, *Geophys. Res. Lett.*, 33,
574 L18402, doi:10.1029/2006GL027657.

- 575 Zhang, L. Hickel, K., Dawes, W.R., Chiew, F., and Western, A. (2004). A rational function approach
576 for estimating mean annual evapotranspiration. *Water Resources Research*, 40, W02502,
577 doi:10.1029/2003WR002710.
- 578 Zhang, L., Cheng, L. and Brutsaert, W. (2017). Estimation of land surface evaporation using a
579 generalized nonlinear complementary relationship. *Journal of Geophysical Research – Atmospheres*,
580 122, doi:10.1002/2016JD025936.
- 581 Zhang, L., Dawes, W. R. and Walker, G. R. (2001). The response of mean annual evapotranspiration
582 to vegetation changes at catchment scale, *Water Resour. Res.*, 37, 701–708.
- 583 Zhou, S., Yu, B., Huang, Y., and Wang, G. (2015). The complementary relationship and generation of
584 the Budyko functions, *Geophys. Res. Lett.*, 42, 1781–1790, doi:10.1002/2015GL063511.
- 585
- 586

587 **Appendix 1.** Estimation of Parameter β for the Linear Complementary Function

588

589 The generalized linear complementary function (9), with E_{po} replaced by βE_e , relating the
 590 actual with the apparent potential evaporation can be written as

$$591 \quad \frac{E}{E_{pa}} = \left[(1+b)\beta \frac{E_e}{E_{pa}} - 1 \right] / b \quad (20)$$

592 Substitution of (7) with $E_{\max} = E_{pa}$ into equation (20) leads to

$$593 \quad \beta = \frac{E_{pa}}{E_e} \left\{ 1 + \frac{b}{1+b} \left[\frac{P}{E_{pa}} - \left[1 + \left(\frac{P}{E_{pa}} \right)^w \right]^{1/w} \right] \right\} \quad (21)$$

594 or concisely

$$595 \quad \beta = \left\{ 1 + c \left[\Phi - (1 + \Phi^w)^{1/w} \right] \right\} / \Psi \quad (22)$$

596 where $\Psi = E_e / E_{pa}$, $\Phi = P / E_{pa} (= AI^{-1})$, and $c = b / (b + 1)$ in which $b = 4.5$, following

597 Brutsaert (2015, Fig. 1). Interestingly, a few trial computations with (21) or (22) have shown

598 that the results are quite close to those obtained herein with (19).